Developmental Cognitive Neuroscience 36 (2019) 100624

Contents lists available at ScienceDirect

Developmental Cognitive Neuroscience

journal homepage: www.elsevier.com/locate/dcn

Applying microstructural models to understand the role of white matter in cognitive development

Elizabeth Huber[a,*], Rafael Neto Henriques[b], Julia P. Owen[c], Ariel Rokem[d], Jason D. Yeatman[a]

[a] Institute for Learning & Brain Sciences and Department of Speech and Hearing Sciences, University of Washington, Seattle, WA, 98195, United States
[b] Champalimaud Neuroscience Programme, Champalimaud Centre for the Unknown, Lisbon, Portugal
[c] Department of Radiology, University of Washington, Seattle, WA, 98195, United States
[d] eScience Institute, University of Washington, Seattle, WA, 98195, United States

ARTICLE INFO

Keywords:
Diffusion MRI
Development
Reading
Dyslexia

ABSTRACT

Diffusion MRI (dMRI) holds great promise for illuminating the biological changes that underpin cognitive development. The diffusion of water molecules probes the cellular structure of brain tissue, and biophysical modeling of the diffusion signal can be used to make inferences about specific tissue properties that vary over development or predict cognitive performance. However, applying these models to study development requires that the parameters can be reliably estimated given the constraints of data collection with children. Here we collect repeated scans using a typical multi-shell diffusion MRI protocol in a group of children (ages 7–12) and use two popular modeling techniques to examine individual differences in white matter structure. We first assess scan-rescan reliability of model parameters and show that axon water faction can be reliably estimated from a relatively fast acquisition, without applying spatial smoothing or de-noising. We then investigate developmental changes in the white matter, and individual differences that correlate with reading skill. Specifically, we test the hypothesis that previously reported correlations between reading skill and diffusion anisotropy in the corpus callosum reflect increased axon water fraction in poor readers. Both models support this interpretation, highlighting the utility of these approaches for testing specific hypotheses about cognitive development.

1. Introduction

White matter biology has been studied extensively using invasive techniques in non-human animals (reviewed in (Walhovd et al., 2014)). Models that link biology to non-invasive MRI measurements hold promise for clarifying the maturational trajectory of human white matter and the neurobiological underpinnings of complex cognitive skills, like reading. However, models with increased biological specificity may be less sensitive to individual differences than metrics derived from the diffusion tensor model (De Santis et al., 2014). For these models to have widespread application in developmental cognitive neuroscience, it is important to ascertain whether the parameters derived from these models reliably index individual differences in the white matter of developing children.

Diffusion tensor imaging (DTI) is the most widely used dMRI technique for studying white matter development, owing partially to the fact that the model is easy to fit and highly reliable. DTI has revealed protracted development of the human white matter with development, continuing throughout adolescence and into adulthood (Lebel and Beaulieu, 2011; Mukherjee et al., 2001). However, DTI metrics lack biological specificity. For example, developmental variation in fractional anisotropy (FA) can reflect differences in axonal packing density, caliber, myelination, or spatial coherence, as well as changes in the number, size, and branching of glial cells (Alexander et al., 2007; Basser and Pierpaoli, 1996; De Santis et al., 2014; Jeurissen et al., 2013; Jones et al., 2013; Walhovd et al., 2014).

Two popular modeling approaches for estimating biologically specific properties of the white matter from dMRI data are the “White Matter Tract Integrity” model (WMTI (Fieremans et al., 2011, 2010)) and the “Neurite Orientation Dispersion and Density Imaging” model (NODDI (Zhang et al., 2012)). Although these models makes certain simplifying assumptions, they have been successfully applied to the study of development (Jelescu et al., 2015), aging (Benitez et al., 2014), and white matter pathology (Benitez et al., 2014; Falangola et al., 2014; Fieremans et al., 2013; Guglielmetti et al., 2016; Jelescu et al., 2016; Kelm et al., 2016), and both provide estimates of tissue properties that are compatible with histological measurements (reviewed in (Jelescu and Budde, 2017)). Recently, NODDI has been used to disentangle

* Corresponding author at: Institute for Learning & Brain Sciences, University of Washington, Portage Bay Building, Box 357988, Seattle, WA, 98195, USA.
E-mail address: ehuber@uw.edu (E. Huber).

https://doi.org/10.1016/j.dcn.2019.100624
Received 11 June 2018; Received in revised form 18 December 2018; Accepted 29 January 2019
Available online 01 February 2019

developmental changes related to dispersion versus density of neurites (axonal and/or dendritic processes) over development (Chang et al., 2015; Genc et al., 2017; Kodiweera et al., 2016; Mah et al., 2017) and in infancy (Kunz et al., 2014; Dean et al., 2017). With the successful application of these models in the context of development, they are now beginning to be applied to the study of individual differences in cognition (Chung et al., 2018). To date, these models have not been applied to the study of reading development.

The relationship between individual differences in reading and white matter diffusion properties has been studied extensively using DTI (Wandell and Yeatman, 2013). While this approach has identified several anatomical correlates of skilled reading, it has often produced conflicting and counterintuitive results. For example, correlations between FA and reading skill are consistently reported in a number of anatomical tracts (Ben-Shachar et al., 2007; Vandermosten et al., 2012), however the direction of the correlation – positive versus negative – varies across studies and brain regions (Ben-Shachar et al., 2007; Deutsch et al., 2005; Klingberg et al., 2000; Lebel and Beaulieu, 2011; Niogi and McCandliss, 2006; Vandermosten et al., 2012; Yeatman et al., 2011), suggesting that the diffusion measurements in a given study may be influenced by different biological phenomena with distinct, and potentially opposing, relationships to reading (Yeatman et al., 2012a). Somewhat counter intuitively, a number of studies have reported *higher* FA in the commissural tracts of individuals with lower reading performance. This phenomenon has been attributed to a higher density of interhemispheric connections, i.e., more callosal axons (Dougherty et al., 2007), although it could also, theoretically, reflect reduced axonal dispersion (i.e., more highly skilled readers have more complex, and less coherent, axonal architecture). However, there has been limited opportunity to test hypotheses about the underlying biological mechanisms that drive variation in reading skill.

The goal of the present work is threefold. First, we assess the scan-rescan reliability of biologically specific white matter indices derived from the WMTI and NODDI models in dMRI data collected in a group of children with varying ages (7–12 years) and varying reading levels (including children with dyslexia and typical readers). We show that the derived values in our sample are reliable and reflect reproducible individual differences. Second, we explore how decisions made in preprocessing affect model reliability. We find that image smoothing or de-noising is unnecessary when data are analyzed within individually defined white matter tracts using a robust measure, such as the median, to estimate values within a region of interest. Third, we examine individual differences in white matter maturation and reading skill, and demonstrate that these models can be used to test specific hypotheses about the correlation between reading skill and white matter diffusion properties. These results highlight the potential for novel modeling approaches to enrich our understanding of the biological bases of cognitive development in health and disease.

2. Methods

2.1. Participants

Diffusion MRI and reading measures were collected for 55 children, ranging in age from 7 to 12 years. Each subject completed a series of reading tests, followed by an MRI scanning session. Subjects had a wide range of reading abilities, as assessed using the Woodcock-Johnson Basic Reading composite (untimed word and pseudo word reading accuracy): Age-normed scores ranged from 52 to 121, with a sample standard deviation of 14.084 (population mean = 100, standard deviation = 15). Of these 55 subjects, 19 had repeated scanning sessions, separated by 2 to 8 weeks. These data were used to assess scan-rescan reliability (Pearson's r calculated using mean tract values for session 1 vs. 2).

All participants were native English speakers with normal or corrected-to-normal vision and no history of neurological damage or psychiatric disorder. Subjects were screened using a mock scanner to assess comfort and ability to hold still during the MRI sessions. We obtained written consent from parents, and verbal assent from all child participants. All procedures, including recruitment, consent, and testing, followed the guidelines of the University of Washington Human Subjects Division and were reviewed and approved by the UW Institutional Review Board.

2.2. Diffusion MRI acquisition and pre-processing

All imaging data were acquired using a 3 T Phillips Achieva scanner (Philips, Eindhoven, Netherlands) at the University of Washington Diagnostic Imaging Sciences Center (DISC) using a 32-channel head coil. An inflatable cap minimized head motion, and participants were continuously monitored through a closed circuit camera system.

Diffusion-weighted magnetic resonance imaging (dMRI) data were acquired at 2.0 mm^3 spatial resolution with full brain coverage. Each session consisted of two DWI scans, one with 32 non-collinear directions (b-value = 800 s/mm^2), and a second with 64 non-collinear directions (b-value = 2000 s/mm^2). Each of the DWI scans included 4 volumes without diffusion weighting (b-value = 0), and the TE (85 ms) was held constant across scans. These acquisition values were chosen to optimally estimate both the NODDI and WMTI model parameters. In addition to these data, a scan with 6 non-diffusion-weighted volumes with a reversed phase encoding direction (posterior-anterior) was also collected to correct for EPI distortions due to inhomogeneities in the magnetic field using FSL's *topup* tool (Andersson et al., 2003). Additional pre-processing was carried out using tools in FSL for motion and eddy current correction (Andersson and Sotiropoulos, 2016). Data were manually checked for imaging artifacts and excessive dropped volumes. Given that subject motion can be especially problematic for the interpretation of group differences in dMRI data (Yendiki et al., 2014), data sets with mean slice-by-slice displacement > 0.7 mm were excluded from further analysis. This resulted in a final sample size of 53 subjects. As a quality check, we calculated the signal-to-noise ratio based on the mean signal within a white matter mask divided by the standard deviation of the signal outside of a head mask within the b = 0 images for each subject. The mean SNR was 25.15, with a standard error across subjects of 0.77.

2.3. Model fitting and analysis

Diffusion metrics were estimated using the diffusion kurtosis model (Jensen et al., 2005), as implemented in DIPY (Garyfallidis et al., 2014). Axonal water fraction (AWF) and extra-axonal diffusivities were then estimated using the white matter tract integrity (WMTI) model (Fieremans et al., 2011, 2010), also implemented in DIPY. Following (Chung et al., 2018; Jensen et al., 2005), we restricted our analysis to voxels with high directional diffusion (fractional anisotropy > 0.3), to satisfy the modeling assumption of well-aligned fibers (Jensen et al., 2005). It is common practice to apply spatial smoothing to the DKI data prior to fitting the WMTI model, to reduce the influence of outliers. To minimize partial volume effects, we opted for block-wise non-local means de-noising (Coupe et al., 2008), implemented in DIPY. We also fit the model using raw DKI outputs, to evaluate the overall impact of a de-noising step in our analysis pipeline.

Intra-axonal volume fraction and orientation dispersion indices were estimated using the NODDI model (Zhang et al., 2012), implemented in Matlab. This provided maps of the intra-cellular tissue volume fraction, orientation dispersion, and an isotropic (Viso) CSF fraction across the brain for each subject. To allow a more direct comparison to AWF, which represents the fraction of restricted water relative to the total water within a voxel, we multiplied the intra-cellular tissue volume fraction from the NODDI model by 1-Viso to obtain a voxel volume fraction, ICVF. Since we limited our analysis to voxels within the core of the white matter, the Viso contribution was typically

0 or nearly 0, so this step had a relatively small effect. The orientation dispersion index (ODI) is a mathematically independent metric that quantifies the coherence of fiber orientations, with a low value indicating aligned fibers.

Values from both modeling approaches were then mapped onto fiber tracts identified in each subject's native space using the Automated Fiber Quantification (AFQ) software package (Yeatman et al., 2012a,b), after initial generation of a whole-brain connectome using probabilistic tractography (MRtrix 3.0)) (Tournier et al., 2004) (see https://github.com/yeatmanlab/afq/wiki for documentation). Fiber tracking was carried out on the aligned, distortion corrected, 64-direction (b-value = 2000 s/mm^2) datasets for each subject. After segmentation with AFQ, selected tracts were sampled into 100 evenly spaced nodes, spanning termination points at the gray-white matter boundary. Mean tracts values were estimated using the middle 60% of each tract, to minimize the influence of crossing fibers near cortical terminations, and to avoid potential partial volume effects at the white matter / gray matter border. AWF from the WMTI model and ICVF/ODI from the NODDI model were mapped onto each tract to create a 'Tract Profile'. Here, we depart slightly from the methods described in (Yeatman et al., 2012a,b) and create these profiles by taking the median value at each node, rather than a distance weighted mean, to create a Tract Profile that is robust to outliers (afq.params.fiberWeighting = 'median'). We compare results for median vs. weighted-mean (the default) Tract Profiles in Fig. 2. Statistical analysis was carried out using software written in Matlab.

3. Results

3.1. WMTI and NODDI parameters index reliable individual differences among children

We began by assessing scan-rescan reliability of the NODDI and WMTI parameters in the non-denoised data of a group of 19 children with repeated scanning sessions. As shown in Fig. 1, all parameters were highly reliable: r = 0.79 median reliability for AWF (range = 0.52 to 0.93); r = 0.79 median reliability for ODI (range = 0.63 to 0.87); and r = 0.84 median reliability for ICVF (range = 0.53 to 0.92). Reliability of DTI based metrics was similar: across tracts, median reliability of FA was 0.77 (range 0.46 to 0.86) and median reliability of MD was 0.70 (range 0.23 to 0.80). Fig. 1**a** shows scan re-scan reliability for all tracts, while **1b** further illustrates the reproducibility of DTI, NODDI, and WMTI parameter values for 2 example tracts.

The fitted values for AWF were consistent with previously reported estimates, ranging, for example, from 0.3 to 0.49 in the corpus callosum (Fieremans et al., 2011, 2010; Tang et al., 1997). Median AWF values were 0.31 for the posterior callosal tract (mean of 0.32, S.E.M across subjects of 0.0030). NODDI ICVF was consistently higher across tracts

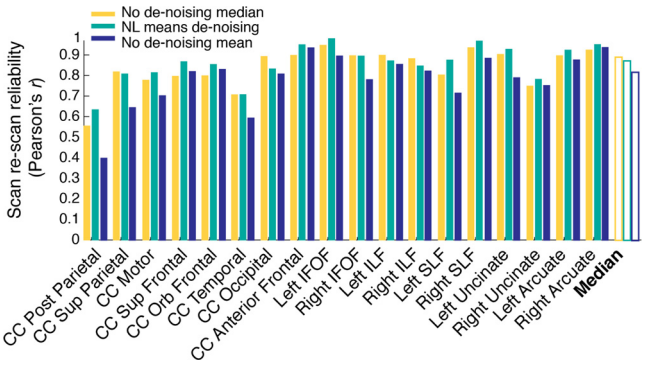

Fig. 2. De-noising has minimal impact on tract-average parameters derived from the WMTI model. Reliability (Pearson's r) calculated for each tract in a group of 19 subjects with repeated scanning sessions. Non-local means filtering was used for image de-noising (see Section 2.3 for details).

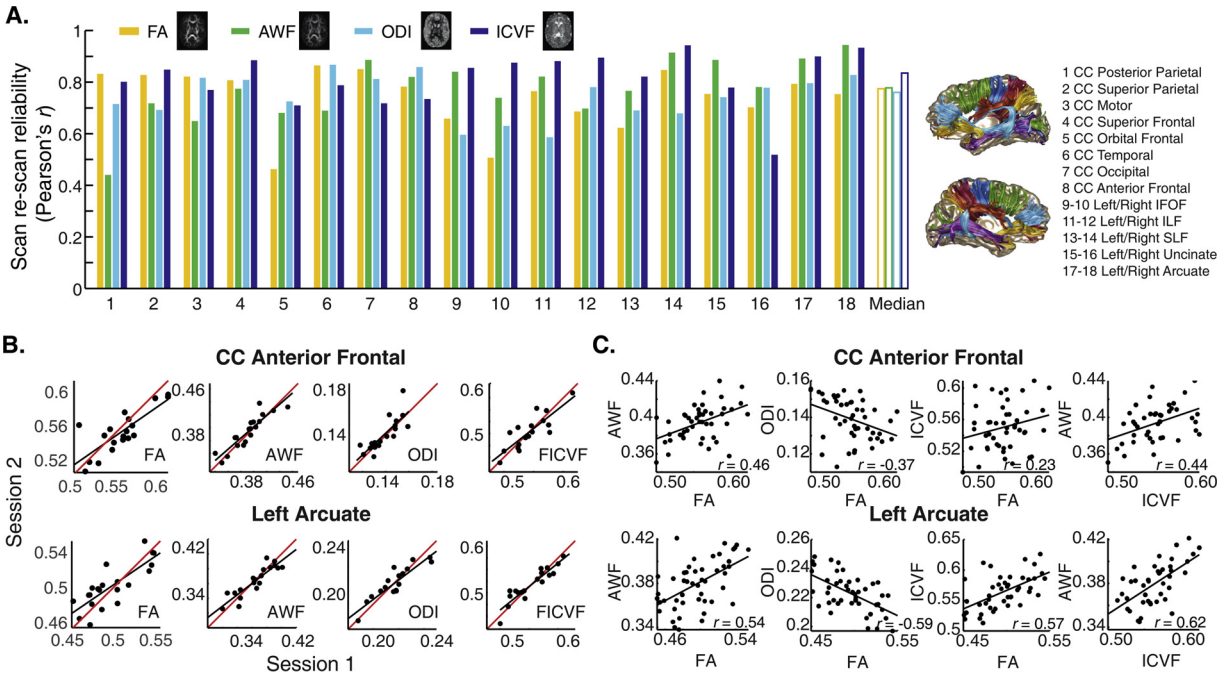

Fig. 1. Parameters are reliable and provide complementary information. (A) Reliability (Pearson's r) in a group of 19 subjects (ranging in age from 8 to 12 years; see Methods) over repeated scanning sessions, separated by 2 to 8 weeks. Median reliability across all tracts (white bars) was greater than r = 0.75 for all three parameters. Example maps are shown for one representative subject, with linear grayscale values ranging from 0 to 1 for each parameter. (B) Scatter plots show tract average axonal water fraction (AWF), intra-cellular volume fraction (ICVF), and orientation dispersion indices (ODI) for all subjects and two example tracts, estimated in Session 1 vs. Session 2. The identity line is shown in red; the line of best fit is shown in black for each plot. (C) Correlations between parameters from DTI, WMTI, and NODDI for the full sample (n = 53) in two example tracts. (For interpretation of the references to colour in this figure legend, the reader is referred to the web version of this article).

Table 1
Correlations among all parameters for each tract, based on the tract average values for all subjects (n = 53).

Tract	FAxAWF	FAxICVF	FAxODI	AWFxICVF
Left IFOF	0.51	0.65	−0.61	0.54
Right IFOF	0.43	0.45	−0.31	0.48
Left ILF	0.65	0.73	−0.28	0.53
Right ILF	0.65	0.57	−0.27	0.58
Left SLF	0.36	0.60	−0.44	0.30
Right SLF	0.72	0.63	−0.41	0.58
Left Unc	0.46	0.71	−0.74	0.46
Right Unc	0.54	0.58	−0.72	0.32
Left Arc	0.54	0.59	−0.59	0.60
Right Arc	0.59	0.53	−0.62	0.59
CC Occiptal	0.71	0.88	−0.87	0.70
CC Anterior	0.47	0.55	−0.37	0.54
CC_Post_Parietal	0.47	0.70	−0.76	0.46
CC_Sup_Parietal	0.59	0.64	−0.78	0.56
CC_Motor	0.69	0.66	−0.70	0.62
CC_Sup_Frontal	0.31	0.50	−0.65	0.45
CC_Orb_Frontal	0.59	0.59	−0.63	0.59
CC_Temporal	0.82	0.78	−0.64	0.75

(as also noted previously, by (Jelescu et al., 2015)): Median ICVF was 0.54 in the posterior callosal tract (mean of 0.53, S.E.M across subjects of 0.0033). Median ODI was 0.15 for the callosal tract (mean 0.17, S.E.M. of 0.0043). This latter value is consistent with previous estimates based on dMRI and histology (Mollink et al., 2017). As expected, ODI values were slightly higher (0.2-0.3) for the association tracts.

Finally, to examine the extent to which different model parameters index similar underlying features of the white matter, we computed correlations between parameters from DTI, WMTI, and NODDI models. Correlations between FA and ICVF, ODI, and AWF, respectively, ranged from 0.45 to 0.73, from -0.27 to -0.74, and 0.36 to 0.72. Tract average values are shown for two example tracts in Fig. 1**c.** Correlations among all parameters for each tract are given in Table 1. Despite high scan rescan reliability, correlations among parameters were modest, on average, consistent with the idea that the different modeling techniques provide unique and complementary anatomical information.

3.2. Anatomically informed robust averaging substitutes for image de-noising

A low signal-to-noise ratio and presence outliers are of particular concern in developmental datasets since the time constraints associated with scanning children often precludes repeated scans within a session, and since these data sets are vulnerable to artifacts from motion and other factors. De-noising is a common additional pre-processing step prior to WMTI model fitting and it is thought to be important for improving the SNR of the data and reducing the influence of outliers in the DKI fits (Jelescu et al., 2015; Veraart et al., 2013). However, researchers are often faced with a challenge when trying to select the necessary and optimal de-noising steps for their data. To analyze the effects of de-noising on scan-rescan reliability, we preprocessed our data using a non-local means filtering approach with commonly used parameter settings (as described in Section 2.3), and without de-noising. As shown in Fig. 2, use of de-noising filter had a minimal influence on the results when median values were extracted from each white matter tract using AFQ. De-noising produced highly reliable estimates, but the reliability was not higher than the non-denoised data. Given the trend for the median reliability to be slightly higher without de-noising, we opted to carry out the rest of our analyses using the non-denoised data set.

While this result might seem counter-intuitive – de-noising does not improve the scan-rescan reliability of parameter estimates – it makes sense in the context of a tract-based analysis (i.e., tractometry) where values are averaged over anatomically defined regions of interest. By using AFQ to extract median values from each white matter tract, we were able to alleviate the need for a de-noising step, since median values are inherently robust to outliers. For comparison, reliabilities are plotted for the non-denoised data sampling the core of the white matter using a using a distance weighted means approach (Yeatman et al., 2012a,b). Reliability is substantially better when values are calculated by taking the median, rather than the weighted-mean, of voxels in a tract, because outlier voxels with extreme values do not bias the median.

3.3. Developmental changes in white matter biology

Developmental changes in mean diffusivity and fractional anisotropy (FA) have been described throughout the white matter (Lebel and Beaulieu, 2011), and there has been recent interest in elaborating these results using biophysical modeling (Chang et al., 2015; Genc et al., 2017; Mah et al., 2017). Here, we begin by examining developmental effects in the posterior callosal connections. We chose this as our target for three reasons. First, the high coherence of axons within the posterior callosal connections should allow for the most accurate estimates of axon properties based on the WMTI model, since the model is less interpretable in regions with complex fiber geometry. Second, histological studies in non-human primates (Hopkins and Phillips, 2010) and structural MRI studies in humans (Giedd et al., 1999, 1996; Kim et al., 2007) indicate that the corpus callosum continues to develop and myelinate throughout childhood and into adolescence, and diffusion properties show large maturational effects within the age range of our sample (McLaughlin et al., 2007; Snook et al., 2005). Finally, the posterior callosum plays a particularly important role in the literature relating DTI measures to reading skills (Dougherty et al., 2007).

As shown in Fig. 3a, ICVF and AWF both increase as a function of age in this tract, while ODI declines. Thus, previously reported variation in FA likely reflects at least two distinct phenomena: Both the increase in AWF/ICVF and the decrease in ODI would contribute to an increase in FA during childhood.

We then carried out an exploratory analysis including all of the commissural and association tracts. We summarize the results of that analysis in Fig. 3**b**. In general, ODI decreased as a function of age, while ICVF and AWF increased, and effect sizes varied across tracts. ICVF increased with age bilaterally in the in the posterior callosal tracts ($p < 0.05$, Bonferroni corrected) and the inferior longitudinal fasciculus and superior frontal callosal tracts ($p < 0.05$, uncorrected). ICVF also increased in the left arcuate fasciculus and inferior frontal fasciculus, and in the right superior longitudinal fasciculus ($p < 0.05$, uncorrected). AWF increased in most tracts measured (all but the anterior callosal connections; $p < 0.05$, uncorrected), with strongest effects in the left and right arcuate and ILF and the anterior and parietal callosal connections ($p < 0.05$, Bonferroni corrected). Meanwhile, ODI decreased in a few callosal tracts – the posterior, superior parietal and motor tracts – and in the right uncinate, but was otherwise stable. All of these effects held in a complementary analysis that included motion as a covariate, alongside age.

3.4. Biological underpinnings of reading-diffusion correlations

The structure of the posterior corpus callosum has previously been shown to vary systematically with reading skill (Dougherty et al., 2007; Frye et al., 2008; Hasan et al., 2012; Odegard et al., 2009), a finding which we replicate here (Fig. 4). We further examined the relationship between NODDI ICVF, NODDI ODI, and WMTI AWF values and reading skills in the same region.

As shown in Fig. 5, ICVF and AWF both significantly correlate with reading skill (Pearson's *r*), while ODI does not. Although we report standardized reading scores, it is possible that confounding effects of age might exist since, for example, older struggling readers often have lower standardized reading scores (i.e., lower scores relative to their

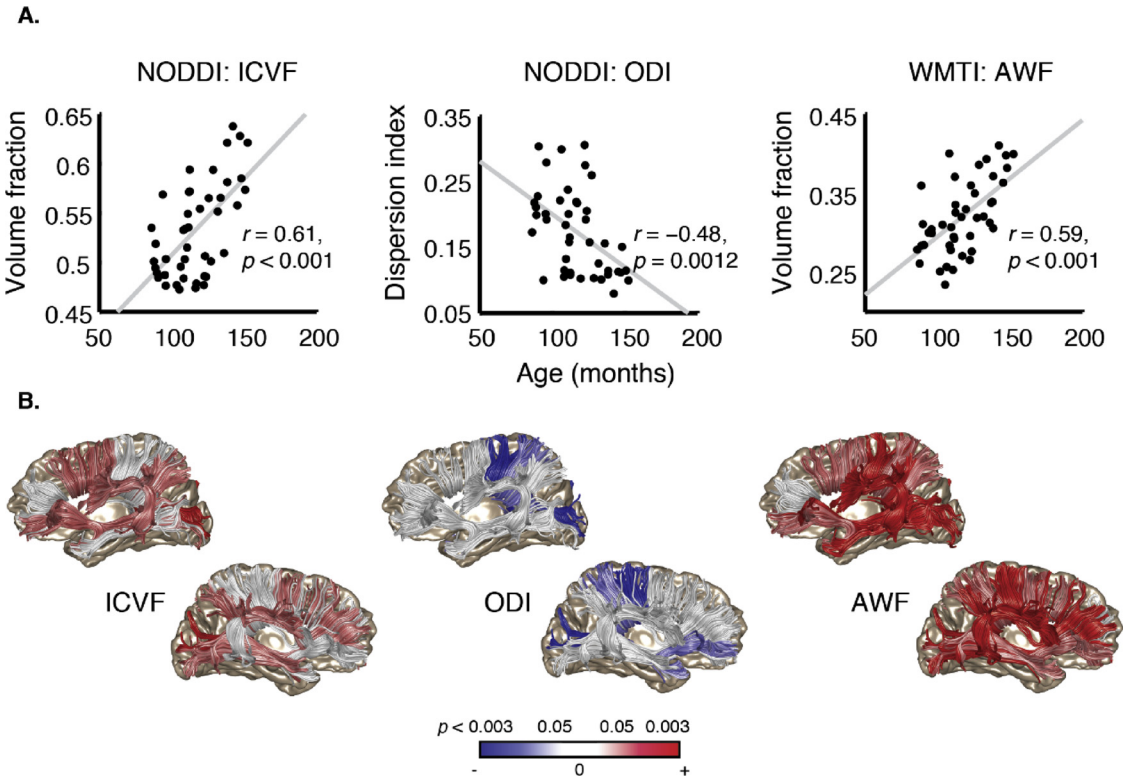

Fig. 3. Developmental changes in the callosal connections and association tracts. (A) Tract average AWF, ODI, and ICVF values plotted as a function of age (in months) for the posterior callosal connections. (B) Anatomical rendering, with tracts showing significant ($p < 0.05$, Bonferroni corrected) age related variation in ICVF, ODI, or AWF highlighted in red (positive correlation) or blue (negative correlation). Tracts rendered in less saturated red and blue show moderate age-related variation ($p < 0.05$, uncorrected). (For interpretation of the references to colour in this figure legend, the reader is referred to the web version of this article).

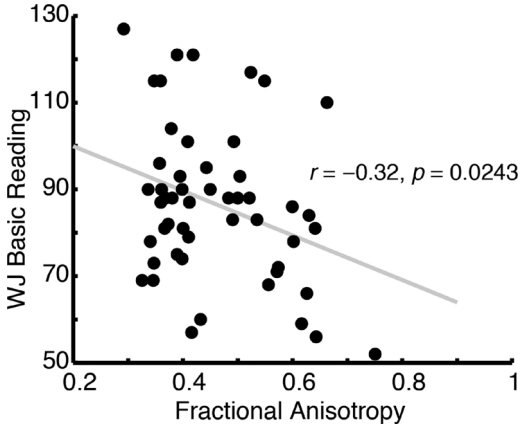

Fig. 4. Fractional anisotropy (FA) in the posterior callosum is negatively correlated with reading skill. Woodcock-Johnson Basic Reading scores are plotted as a function of tract average FA values from the posterior callosal connections. Replicating previous studies, we find a negative relationship between FA and reading skill within this region: Individuals with higher FA are generally worse readers.

peers). To control for a possible confounding effects of age, given the age dependence of the NODDI and WMTI parameters, we fit a linear model predicting reading scores from each parameter with age included as a covariate. In this analysis, NODDI ICVF accounted for a significant proportion of the variance in reading skill ($F(1,41) = 5.33$, $p = 0.026$). Meanwhile, NODDI ODI was not a significant predictor of reading skill, over and above age: $F(1,41) = 1.33$, $p = 0.25$. In line with this result, AWF also predicted reading skill, over and above age: $F(1,43) = 6.14$, $p = 0.017$. Including motion as a covariate did not change these results ($p = 0.014$, 0.13, and 0.0069, respectively).

Finally, we carried out an exploratory analysis of each additional tract in the data set, using the average value along each tract, as above. As shown in Fig. 5, only ICVF in the anterior callosal tract and ODI in the right arcuate significantly predicted reading skill, after controlling for age. Thus, the correlation between axon properties and reading skill was relatively specific to the posterior callosum in this sample. To further examine the relationship between reading skill and the structure of the posterior callosal tract, we divided the subjects into two groups: "skilled" readers (n = 29) with a basic reading score within a single standard deviation of the population average, and "struggling readers" (n = 24) with a basic reading score below that level (1 SD below the population mean is a typical cutoff for defining dyslexia (see Rimrodt et al., 2009; Shaywitz et al., 2002; Kubota et al., 2018). As shown in Fig. 5**c**, the struggling readers tended to have higher ICVF along the entire posterior callosal tract.

4. Discussion

Here we use two popular modeling techniques, "White Matter Tract Integrity" or WMTI (Fieremans et al., 2011, 2010) and "Neurite Orientation Dispersion and Density Imaging" or NODDI, to examine white matter properties related to development and individual differences in reading skill in a group of grade-school aged children. Both models provided metrics that were reliable and within the expected range based on previous estimates from histology and in vivo microscopy (reviewed in (Jelescu and Budde, 2017)). We then used the AFQ tractometry pipeline to generate anatomically informed, robust estimates of model parameters for each tract without prior image denoising. We note, however, that data with relatively low signal-to-noise might still benefit from a denoising step and that denoising might be necessary for a voxel-wise analysis. In general, diffusion MRI suffers from relatively low signal-to-noise ratio, particularly when diffusion weighting is high

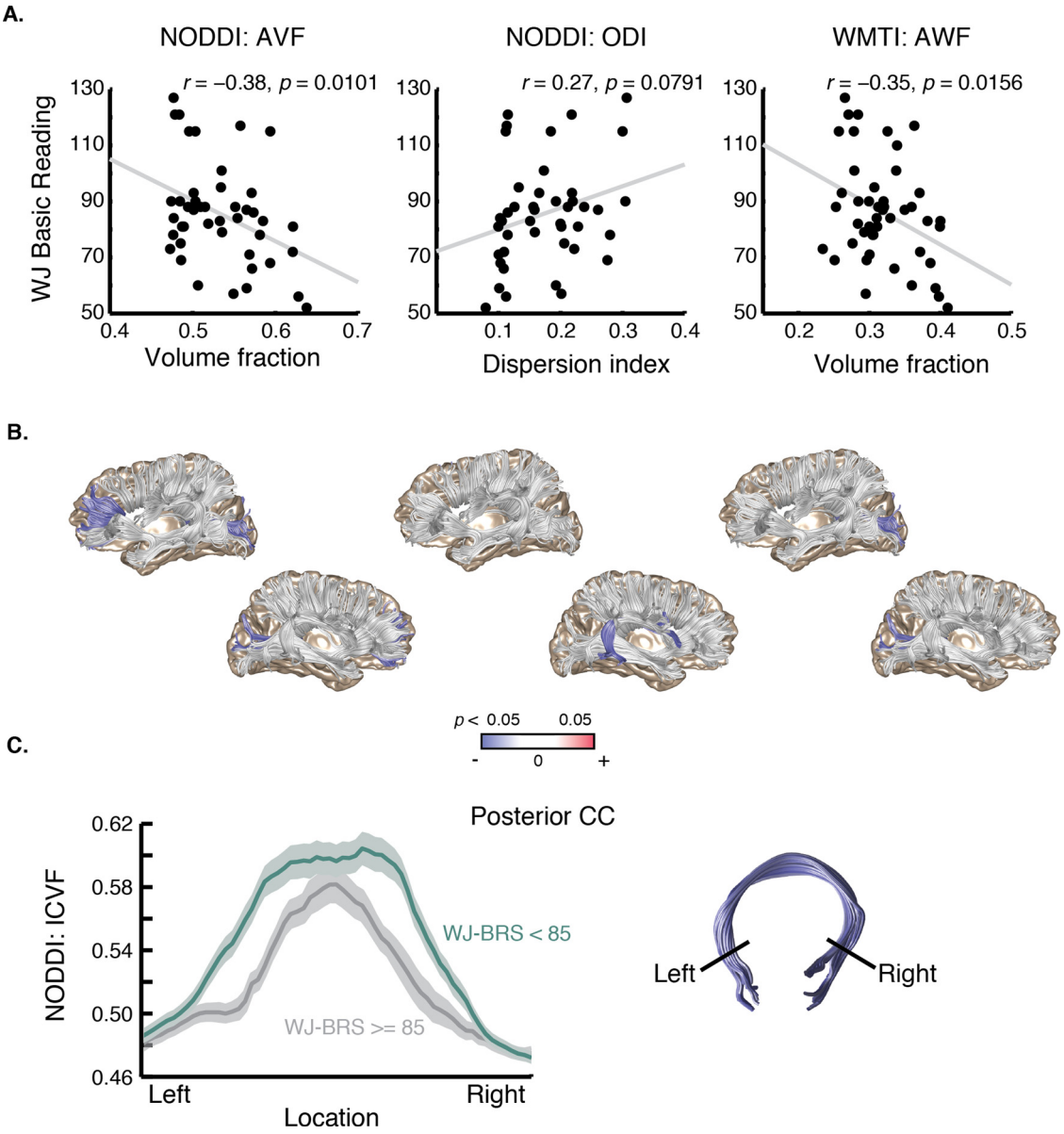

Fig. 5. Indices of tissue density in the posterior callosal connections correlate with reading skill. (A) Scatter plot showing Basic Reading as a function of tract average NODDI ICVF, ODI, and WMTI AWF values. Insets show tract profiles for skilled vs. struggling readers for each parameter (mean +/- 1 standard error). (B) Anatomical rendering, with tracts showing significant ($p < 0.05$) reading related variation, after controlling for age, ICVF, ODI, or AWF highlighted in red. (C) Tract profile along the posterior callosal connections showing mean ICVF for skilled readers (WJ Basic Reading score at or above 85) and struggling readers (WJ Basic Reading score below 85). The x-axis spans the middle 60% of each tract the where it was clipped prior to analysis (corresponding to black boundary lines in the example anatomical renderings, at right). Shading represents one standard error of the mean. The locations of individual nodes showing a significant group difference in a *t*-test ($p < 0.05$) are shown along the x-axis in red (For interpretation of the references to colour in this figure legend, the reader is referred to the web version of this article).

(larger b-values) (Jones and Basser, 2004), and so it is important to examine the influence of noise to determine the optimal preprocessing steps for a given dataset. Finally, we used the estimated parameters from each model to examine age- and reading skill-related variation in white matter properties, highlighting the utility of these models for testing specific hypotheses about the biology of the white matter in relation to cognitive development.

Model-estimated axonal water fraction (AWF) and intra-cellular volume fraction (ICVF) increased linearly with age in a large collection of anatomical tracts. ICVF increased with age bilaterally in the inferior longitudinal fasciculus and the posterior and superior frontal callosal tracts. ICVF also increased in the left arcuate fasciculus and inferior frontal fasciculus, and in the right superior longitudinal fasciculus. AWF increased in nearly every tract measured. Meanwhile, ODI decreased in a few callosal tracts – the posterior, superior parietal and motor tracts – and in the right uncinate, but was otherwise stable. Together, these factors should contribute to a widespread developmental increase in FA, as reported elsewhere (Lebel and Beaulieu, 2011). A recent study examining FA and NODDI metrics showed a similar pattern: On average, cortical tracts show relatively stable ODI during the first decade of life, with a gradual increase that accelerates over the lifespan, while neurite density increases sharply (Chang et al., 2015). These findings are consistent with the idea that developmental changes in white matter diffusion primarily reflect changes in axonal number/density or myelination, since the former would influence ICVF and AWF directly by changing the fraction of water restricted within axons, while the latter would influence these parameters indirectly by reducing the volume of the extra-axonal space. In contrast, although ODI does not

vary over development in our sample, individual values were reproducible across scanning sessions, suggesting that this parameter captures stable individual variation in white matter organization.

Although AWF and ICVF both increased over development in the posterior callosal connections, these properties also varied as a function of reading skill, independent of age. The structure of the posterior corpus callosum has previously been shown to differ in both children and adults with dyslexia (Duara et al., 1991; Rumsey et al., 1996; von Plessen et al., 2002v), and several studies have reported correlations between reading-related skills and diffusion properties within posterior callosal regions (Dougherty et al., 2007; Frye et al., 2008; Hasan et al., 2012; Odegard et al., 2009). In the diffusion literature, higher radial diffusivity and lower FA for this tract have been associated with higher reading proficiency. These effects are somewhat counter intuitive, given that they would suggest reduced density of inter-hemispheric connections in strong readers, but they have been linked to the hypothesis that reading-related functions are not as strongly left-lateralized in struggling readers (Finn et al., 2014; Galaburda et al.,1986; Galaburda et al., 1985). Higher tissue density (for example, more densely packed or more heavily myelinated axons) in this region in struggling readers could account for this effect, as hypothesized by (Ben-Shachar et al., 2007). However, reduced axonal dispersion could also account for the higher FA. Using the WMTI and NODDI models, we were able to examine these possibilities: We found that axonal water fraction and intra-cellular volume fraction of the posterior callosal tract correlate with reading skill, while orientation dispersion does not.

Given the stable relationship between reading ability and the structure of posterior callosal connections, it is plausible that differences in axonal properties within this region may emerge early in life and influence subsequent development throughout the reading circuitry, even as the callosal connections themselves continue to mature. In line with this hypothesis, the posterior callosal tract was remarkably stable within subjects during an 8-week, intensive reading intervention that prompted large changes in diffusion properties throughout a collection of cortical association and projection tracts (Huber et al., 2018). Indeed the callosum was one of just a few tracts that did not change during the intensive reading skills training program. Thus, anatomical differences that are stabilized prior to age 7 (the youngest individuals included in our sample) in the posterior callosal tract may ultimately shape reading development, while other portions of the reading network remain amenable to change, perhaps reflecting compensatory mechanisms that can emerge with educational intervention (Barquero et al., 2014; Eden et al., 2004; Hoeft et al., 2011; Shaywitz et al., 2004). Future work linking white matter biology to functional responses within the reading circuitry should help to build a more nuanced view of the computations involved, and the ways in which these circuits develop and adapt to experience.

5. Conclusions

Advanced modeling techniques offer a bridge between diffusion MRI and histology, allowing us to test specific, biologically based hypotheses about cognitive development. If data processing steps are taken to ensure reliable parameter estimates, this approach holds promise for adding nuance to our understanding of the biological changes that occur in human white matter over development and for revealing the computational mechanisms associated with individual differences in cognition.

Declarations of interest

None.

Acknowledgements

This work was funded by NSF/BSF BCS #1551330 to JDY. The International Neuroinformatics Coordinating Facility (INCF) provided support through a project and travel grant to RNH. AR was funded through a grant from the Gordon & Betty Moore Foundation and the Alfred P. Sloan Foundation to the University of Washington eScience Institute.

References

Alexander, A.L., Lee, J.E., Lazar, M., Field, A.S., 2007. Diffusion tensor imaging of the brain. Neurotherapeutics 4 (3), 316–329. https://doi.org/10.1016/j.nurt.2007.05.011.

Andersson, J.L., Sotiropoulos, S.N., 2016. An integrated approach to correction for off-resonance effects and subject movement in diffusion MR imaging. Neuroimage 125, 1063–1078. https://doi.org/10.1016/j.neuroimage.2015.10.019.

Andersson, J.L., Skare, S., Ashburner, J., 2003. How to correct susceptibility distortions in spin-echo echo-planar images: application to diffusion tensor imaging. Neuroimage 20 (2), 870–888. https://doi.org/10.1016/S1053-8119(03)00336-7.

Barquero, L.A., Davis, N., Cutting, L.E., 2014. Neuroimaging of reading intervention: a systematic review and activation likelihood estimate meta-analysis. PLoS One 9 (1), e83668. https://doi.org/10.1371/journal.pone.0083668.

Basser, P.J., Pierpaoli, C., 1996. Microstructural and physiological features of tissues elucidated by quantitative-diffusion-tensor MRI. J. Magn. Reson. B 111 (3), 209–219.

Benitez, A., Fieremans, E., Jensen, J.H., Falangola, M.F., Tabesh, A., Ferris, S.H., Helpern, J.A., 2014. White matter tract integrity metrics reflect the vulnerability of late-myelinating tracts in Alzheimer's disease. Neuroimage Clin 4, 64–71. https://doi.org/10.1016/j.nicl.2013.11.001.

Ben-Shachar, M., Dougherty, R.F., Wandell, B.A., 2007. White matter pathways in reading. Curr. Opin. Neurobiol. 17 (2), 258–270. https://doi.org/10.1016/j.conb.2007.03.006.

Chang, Y.S., Owen, J.P., Pojman, N.J., Thieu, T., Bukshpun, P., Wakahiro, M.L., et al., 2015. White matter changes of neurite density and fiber orientation dispersion during human brain maturation. PLoS One 10 (6), e0123656. https://doi.org/10.1371/journal.pone.0123656.

Chung, S., Fieremans, E., Kucukboyaci, N.E., Wang, X., Morton, C.J., Novikov, D.S., et al., 2018. Working memory and brain tissue microstructure: white matter tract integrity based on multi-shell diffusion MRI. Sci. Rep. 8 (1), 3175. https://doi.org/10.1038/s41598-018-21428-4.

Coupe, P., Yger, P., Prima, S., Hellier, P., Kervrann, C., Barillot, C., 2008. An optimized blockwise nonlocal means denoising filter for 3-D magnetic resonance images. IEEE Trans. Med. Imaging 27 (4), 425–441. https://doi.org/10.1109/TMI.2007.906087.

Dean, Douglas C., et al., 2017. Investigation of brain structure in the 1-month infant. Brain Struct. Funct. 223, 1953–1970.

De Santis, S., Drakesmith, M., Bells, S., Assaf, Y., Jones, D.K., 2014. Why diffusion tensor MRI does well only some of the time: variance and covariance of white matter tissue microstructure attributes in the living human brain. Neuroimage 89, 35–44. https://doi.org/10.1016/j.neuroimage.2013.12.003.

Deutsch, G.K., Dougherty, R.F., Bammer, R., Siok, W.T., Gabrieli, J.D., Wandell, B., 2005. Children's reading performance is correlated with white matter structure measured by diffusion tensor imaging. Cortex 41 (3), 354–363.

Dougherty, R.F., Ben-Shachar, M., Deutsch, G.K., Hernandez, A., Fox, G.R., Wandell, B.A., 2007. Temporal-callosal pathway diffusivity predicts phonological skills in children. Proc. Natl. Acad. Sci. U. S. A. 104 (20), 8556–8561. https://doi.org/10.1073/pnas.0608961104.

Duara, R., Kushch, A., Gross-Glenn, K., Barker, W.W., Jallad, B., Pascal, S., et al., 1991. Neuroanatomic differences between dyslexic and normal readers on magnetic resonance imaging scans. Arch. Neurol. 48 (4), 410–416.

Eden, G.F., Jones, K.M., Cappell, K., Gareau, L., Wood, F.B., Zeffiro, T.A., et al., 2004. Neural changes following remediation in adult developmental dyslexia. Neuron 44 (3), 411–422. https://doi.org/10.1016/j.neuron.2004.10.019.

Falangola, M.F., Guilfoyle, D.N., Tabesh, A., Hui, E.S., Nie, X., Jensen, J.H., et al., 2014. Histological correlation of diffusional kurtosis and white matter modeling metrics in cuprizone-induced corpus callosum demyelination. NMR Biomed. 27 (8), 948–957. https://doi.org/10.1002/nbm.3140.

Fieremans, E., Novikov, D.S., Jensen, J.H., Helpern, J.A., 2010. Monte Carlo study of a two-compartment exchange model of diffusion. NMR Biomed. 23 (7), 711–724. https://doi.org/10.1002/nbm.1577.

Fieremans, E., Jensen, J.H., Helpern, J.A., 2011. White matter characterization with diffusional kurtosis imaging. Neuroimage 58 (1), 177–188. https://doi.org/10.1016/j.neuroimage.2011.06.006.

Fieremans, E., Benitez, A., Jensen, J.H., Falangola, M.F., Tabesh, A., Deardorff, R.L., et al., 2013. Novel white matter tract integrity metrics sensitive to Alzheimer disease progression. AJNR Am J Neuroradiol 34 (11), 2105–2112. https://doi.org/10.3174/ajnr.A3553.

Finn, E.S., Shen, X., Holahan, J.M., Scheinost, D., Lacadie, C., Papademetris, X., et al., 2014. Disruption of functional networks in dyslexia: a whole-brain, data-driven analysis of connectivity. Biol. Psychiatry 76 (5), 397–404. https://doi.org/10.1016/j.biopsych.2013.08.031.

Frye, R.E., Hasan, K., Xue, L., Strickland, D., Malmberg, B., Liederman, J., Papanicolaou, A., 2008. Splenium microstructure is related to two dimensions of reading skill. Neuroreport 19 (16), 1627–1631. https://doi.org/10.1097/WNR.0b013e328314b8ee.

Galaburda, A.M., Sherman, G.F., Rosen, G.D., Aboitiz, F., Geschwind, N., 1985. Developmental dyslexia: four consecutive patients with cortical anomalies. Ann.

Neurol. 18 (2), 222–233. https://doi.org/10.1002/ana.410180210.
Galaburda, A.M., Aboitiz, F., Rosen, G.D., Sherman, G.F., 1986. Histological asymmetry in the primary visual cortex of the rat: implications for mechanisms of cerebral asymmetry. Cortex 22 (1), 151–160.
Garyfallidis, E., Brett, M., Amirbekian, B., Rokem, A., van der Walt, S., Descoteaux, M., et al., 2014. Dipy, a library for the analysis of diffusion MRI data. Front Neuroinform 8, 8. https://doi.org/10.3389/fninf.2014.00008.
Genc, S., Malpas, C.B., Holland, S.K., Beare, R., Silk, T.J., 2017. Neurite density index is sensitive to age related differences in the developing brain. Neuroimage 148, 373–380. https://doi.org/10.1016/j.neuroimage.2017.01.023.
Giedd, J.N., Rumsey, J.M., Castellanos, F.X., Rajapakse, J.C., Kaysen, D., Vaituzis, A.C., et al., 1996. A quantitative MRI study of the corpus callosum in children and adolescents. Brain Res. Dev. Brain Res. 91 (2), 274–280.
Giedd, J.N., Blumenthal, J., Jeffries, N.O., Rajapakse, J.C., Vaituzis, A.C., Liu, H., et al., 1999. Development of the human corpus callosum during childhood and adolescence: a longitudinal MRI study. Prog. Neuropsychopharmacol. Biol. Psychiatry 23 (4), 571–588.
Guglielmetti, C., Veraart, J., Roelant, E., Mai, Z., Daans, J., Van Audekerke, J., et al., 2016. Diffusion kurtosis imaging probes cortical alterations and white matter pathology following cuprizone induced demyelination and spontaneous remyelination. Neuroimage 125, 363–377. https://doi.org/10.1016/j.neuroimage.2015.10.052.
Hasan, K.M., Molfese, D.L., Walimuni, I.S., Stuebing, K.K., Papanicolaou, A.C., Narayana, P.A., Fletcher, J.M., 2012. Diffusion tensor quantification and cognitive correlates of the macrostructure and microstructure of the corpus callosum in typically developing and dyslexic children. NMR Biomed. 25 (11), 1263–1270. https://doi.org/10.1002/nbm.2797.
Hoeft, F., McCandliss, B.D., Black, J.M., Gantman, A., Zakerani, N., Hulme, C., et al., 2011. Neural systems predicting long-term outcome in dyslexia. Proc. Natl. Acad. Sci. U. S. A. 108 (1), 361–366. https://doi.org/10.1073/pnas.1008950108.
Hopkins, W.D., Phillips, K.A., 2010. Cross-sectional analysis of the association between age and corpus callosum size in chimpanzees (Pan troglodytes). Dev. Psychobiol. 52 (2), 133–141. https://doi.org/10.1002/dev.20421.
Huber, E., Donnelly, P.M., Rokem, A., Yeatman, J.D., 2018. Rapid and widespread white matter plasticity during an intensive reading intervention. Nat. Commun.
Jelescu, I.O., Budde, M.D., 2017. Design and validation of diffusion MRI models of white matter. Front. Phys. 28. https://doi.org/10.3389/fphy.2017.00061.
Jelescu, I.O., Veraart, J., Adisetiyo, V., Milla, S.S., Novikov, D.S., Fieremans, E., 2015. One diffusion acquisition and different white matter models: how does microstructure change in human early development based on WMTI and NODDI? Neuroimage 107, 242–256. https://doi.org/10.1016/j.neuroimage.2014.12.009.
Jelescu, I.O., Zurek, M., Winters, K.V., Veraart, J., Rajaratnam, A., Kim, N.S., et al., 2016. In vivo quantification of demyelination and recovery using compartment-specific diffusion MRI metrics validated by electron microscopy. Neuroimage 132, 104–114. https://doi.org/10.1016/j.neuroimage.2016.02.004.
Jensen, J.H., Helpern, J.A., Ramani, A., Lu, H., Kaczynski, K., 2005. Diffusional kurtosis imaging: the quantification of non-gaussian water diffusion by means of magnetic resonance imaging. Magn. Reson. Med. 53 (6), 1432–1440. https://doi.org/10.1002/mrm.20508.
Jeurissen, B., Leemans, A., Tournier, J.D., Jones, D.K., Sijbers, J., 2013. Investigating the prevalence of complex fiber configurations in white matter tissue with diffusion magnetic resonance imaging. Hum. Brain Mapp. 34 (11), 2747–2766. https://doi.org/10.1002/hbm.22099.
Jones, Derek K., Basser, Peter J., 2004. Squashing peanuts and smashing pumpkins: how noise distorts diffusion-weighted MR data. Magn. Reson. Med. 52 (5), 979–993.
Jones, D.K., Knosche, T.R., Turner, R., 2013. White matter integrity, fiber count, and other fallacies: the do's and don'ts of diffusion MRI. Neuroimage 73, 239–254. https://doi.org/10.1016/j.neuroimage.2012.06.081.
Kelm, N.D., West, K.L., Carson, R.P., Gochberg, D.F., Ess, K.C., Does, M.D., 2016. Evaluation of diffusion kurtosis imaging in ex vivo hypomyelinated mouse brains. Neuroimage 124 (Pt A), 612–626. https://doi.org/10.1016/j.neuroimage.2015.09.028.
Kim, E.Y., Kim, D.H., Yoo, E., Park, H.J., Golay, X., Lee, S.K., Kim, D.I., 2007. Visualization of maturation of the corpus callosum during childhood and adolescence using T2 relaxometry. Int. J. Dev. Neurosci. 25 (6), 409–414. https://doi.org/10.1016/j.ijdevneu.2007.05.005.
Klingberg, T., Hedehus, M., Temple, E., Salz, T., Gabrieli, J.D., Moseley, M.E., Poldrack, R.A., 2000. Microstructure of temporo-parietal white matter as a basis for reading ability: evidence from diffusion tensor magnetic resonance imaging. Neuron 25 (2), 493–500.
Kodiweera, C., Alexander, A.L., Harezlak, J., McAllister, T.W., Wu, Y.C., 2016. Age effects and sex differences in human brain white matter of young to middle-aged adults: a DTI, NODDI, and q-space study. Neuroimage 128, 180–192. https://doi.org/10.1016/j.neuroimage.2015.12.033.
Kunz, Nicolas, et al., 2014. Assessing white matter microstructure of the newborn with multi-shell diffusion MRI and biophysical compartment models. NeuroImage 96, 288–299.
Lebel, C., Beaulieu, C., 2011. Longitudinal development of human brain wiring continues from childhood into adulthood. J. Neurosci. 31 (30), 10937–10947. https://doi.org/10.1523/JNEUROSCI.5302-10.2011.
Mah, A., Geeraert, B., Lebel, C., 2017. Detailing neuroanatomical development in late childhood and early adolescence using NODDI. PLoS One 12 (8), e0182340. https://doi.org/10.1371/journal.pone.0182340.
McLaughlin, N.C., Paul, R.H., Grieve, S.M., Williams, L.M., Laidlaw, D., DiCarlo, M., et al., 2007. Diffusion tensor imaging of the corpus callosum: a cross-sectional study across the lifespan. Int. J. Dev. Neurosci. 25 (4), 215–221. https://doi.org/10.1016/j.ijdevneu.2007.03.008.
Mollink, J., Kleinnijenhuis, M., Cappellen van Walsum, A.V., Sotiropoulos, S.N., Cottaar, M., Mirfin, C., et al., 2017. Evaluating fibre orientation dispersion in white matter: comparison of diffusion MRI, histology and polarized light imaging. Neuroimage 157, 561–574. https://doi.org/10.1016/j.neuroimage.2017.06.001.
Mukherjee, P., Miller, J.H., Shimony, J.S., Conturo, T.E., Lee, B.C., Almli, C.R., McKinstry, R.C., 2001. Normal brain maturation during childhood: developmental trends characterized with diffusion-tensor MR imaging. Radiology 221 (2), 349–358. https://doi.org/10.1148/radiol.2212001702.
Niogi, S.N., McCandliss, B.D., 2006. Left lateralized white matter microstructure accounts for individual differences in reading ability and disability. Neuropsychologia 44 (11), 2178–2188. https://doi.org/10.1016/j.neuropsychologia.2006.01.011.
Odegard, T.N., Farris, E.A., Ring, J., McColl, R., Black, J., 2009. Brain connectivity in non-reading impaired children and children diagnosed with developmental dyslexia. Neuropsychologia 47 (8-9), 1972–1977. https://doi.org/10.1016/j.neuropsychologia.2009.03.009.
Rumsey, J.M., Casanova, M., Mannheim, G.B., Patronas, N., De Vaughn, N., Hamburger, S.D., Aquino, T., 1996. Corpus callosum morphology, as measured with MRI, in dyslexic men. Biol. Psychiatry 39 (9), 769–775.
Shaywitz, B.A., Shaywitz, S.E., Blachman, B.A., Pugh, K.R., Fulbright, R.K., Skudlarski, P., et al., 2004. Development of left occipitotemporal systems for skilled reading in children after a phonologically- based intervention. Biol. Psychiatry 55 (9), 926–933. https://doi.org/10.1016/j.biopsych.2003.12.019.
Snook, L., Paulson, L.A., Roy, D., Phillips, L., Beaulieu, C., 2005. Diffusion tensor imaging of neurodevelopment in children and young adults. Neuroimage 26 (4), 1164–1173. https://doi.org/10.1016/j.neuroimage.2005.03.016.
Tang, Y., Nyengaard, J.R., Pakkenberg, B., Gundersen, H.J., 1997. Age-induced white matter changes in the human brain: a stereological investigation. Neurobiol. Aging 18 (6), 609–615.
Tournier, J.D., Calamante, F., Gadian, D.G., Connelly, A., 2004. Direct estimation of the fiber orientation density function from diffusion-weighted MRI data using spherical deconvolution. Neuroimage 23 (3), 1176–1185. https://doi.org/10.1016/j.neuroimage.2004.07.037.
Vandermosten, M., Boets, B., Wouters, J., Ghesquiere, P., 2012. A qualitative and quantitative review of diffusion tensor imaging studies in reading and dyslexia. Neurosci. Biobehav. Rev. 36 (6), 1532–1552. https://doi.org/10.1016/j.neubiorev.2012.04.002.
Veraart, J., Rajan, J., Peeters, R.R., Leemans, A., Sunaert, S., Sijbers, J., 2013. Comprehensive framework for accurate diffusion MRI parameter estimation. Magn. Reson. Med. 70 (4), 972–984. https://doi.org/10.1002/mrm.24529.
von Plessen, K., Lundervold, A., Duta, N., Heiervang, E., Klauschen, F., Smievoll, A.I., et al., 2002v. Less developed corpus callosum in dyslexic subjects–a structural MRI study. Neuropsychologia 40 (7), 1035–1044.
Walhovd, K.B., Johansen-Berg, H., Karadottir, R.T., 2014. Unraveling the secrets of white matter–bridging the gap between cellular, animal and human imaging studies. Neuroscience 276, 2–13. https://doi.org/10.1016/j.neuroscience.2014.06.058.
Wandell, B.A., Yeatman, J.D., 2013. Biological development of reading circuits. Curr. Opin. Neurobiol. 23 (2), 261–268. https://doi.org/10.1016/j.conb.2012.12.005.
Yeatman, J.D., Dougherty, R.F., Rykhlevskaia, E., Sherbondy, A.J., Deutsch, G.K., Wandell, B.A., Ben-Shachar, M., 2011. Anatomical properties of the arcuate fasciculus predict phonological and reading skills in children. J. Cogn. Neurosci. 23 (11), 3304–3317. https://doi.org/10.1162/jocn_a_00061.
Yeatman, J.D., Dougherty, R.F., Ben-Shachar, M., Wandell, B.A., 2012a. Development of white matter and reading skills. Proc. Natl. Acad. Sci. U. S. A. 109 (44), E3045–3053. https://doi.org/10.1073/pnas.1206792109.
Yeatman, J.D., Dougherty, R.F., Myall, N.J., Wandell, B.A., Feldman, H.M., 2012b. Tract profiles of white matter properties: automating fiber-tract quantification. PLoS One 7 (11), e49790. https://doi.org/10.1371/journal.pone.0049790.
Yendiki, A., Koldewyn, K., Kakunoori, S., Kanwisher, N., Fischl, B., 2014. Spurious group differences due to head motion in a diffusion MRI study. Neuroimage 88, 79–90. https://doi.org/10.1016/j.neuroimage.2013.11.027.
Zhang, H., Schneider, T., Wheeler-Kingshott, C.A., Alexander, D.C., 2012. NODDI: practical in vivo neurite orientation dispersion and density imaging of the human brain. Neuroimage 61 (4), 1000–1016. https://doi.org/10.1016/j.neuroimage.2012.03.072.